Science Advances
AAAS

advances.sciencemag.org/cgi/content/full/7/20/eabg1455/DC1

Supplementary Materials for

In-sensor reservoir computing for language learning via two-dimensional memristors

Linfeng Sun, Zhongrui Wang, Jinbao Jiang, Yeji Kim, Bomin Joo, Shoujun Zheng, Seungyeon Lee, Woo Jong Yu, Bai-Sun Kong, Heejun Yang*

*Corresponding author. Email: h.yang@kaist.ac.kr

Published 14 May 2021, *Sci. Adv.* **7**, eabg1455 (2021)
DOI: 10.1126/sciadv.abg1455

The PDF file includes:

Other Supplementary Material for this manuscript includes the following:

(available at advances.sciencemag.org/cgi/content/full/7/20/eabg1455/DC1)

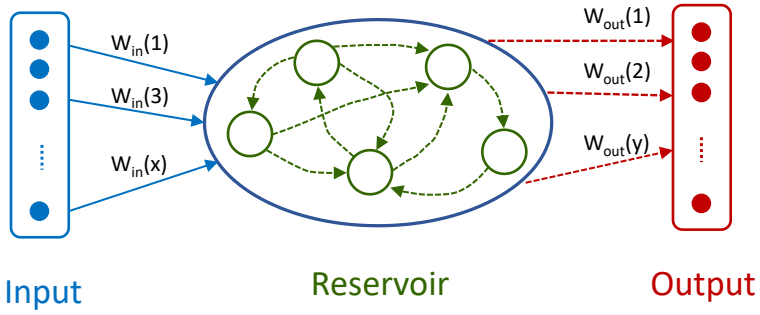

Fig. S1. A typical schematic of a RC system with input signals denoted by the blue circles, a reservoir with internal dynamics (black circles and dashed arrows), and a readout map (red dashed arrows). In the RC system, the weights of connections among the reservoir nodes (black circles) are randomly assigned and fixed, and only the weights connecting the reservoir nodes and the output nodes are trained.

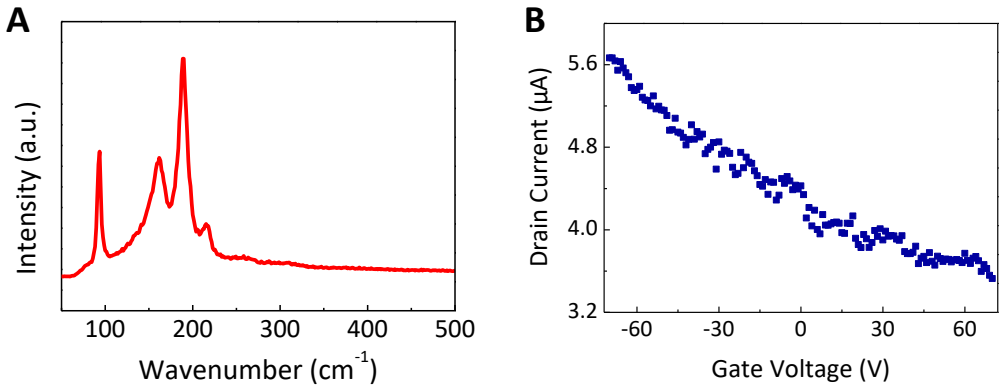

Fig. S2. Optoelectronic characterization of the SnS used in this work. (**A**)The Raman spectrum of the SnS samples shown in Figure 1. I-V sweeps have no impact on the Raman spectrum. The pristine properties of SnS were retained during the operation of the device. (**B**) The I_d-V_g curve of the SnS samples.

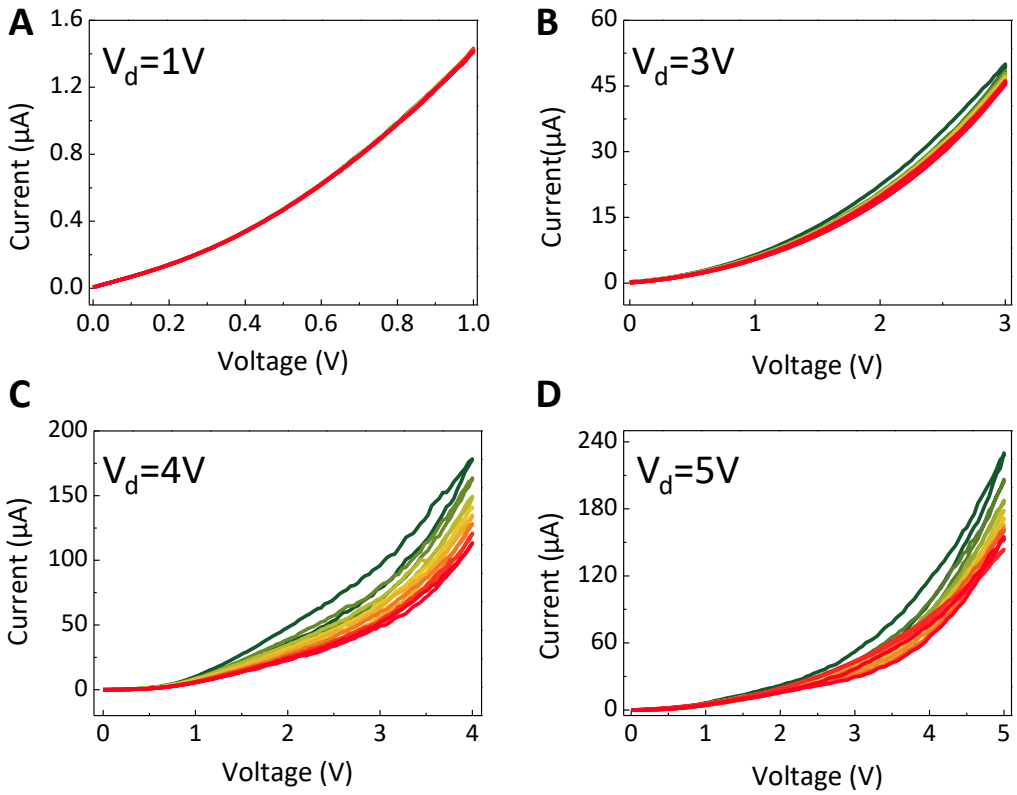

Fig. S3. Bias-voltage-dependent I-V switching curves are presented. Ten cycles are measured for each figure. (**A**) V_d = 1V, (**B**) V_d = 2V, (**C**) V_d = 3V. (**D**) V_d = 4V. V_d refers to the maximum voltage of the I-V curves.

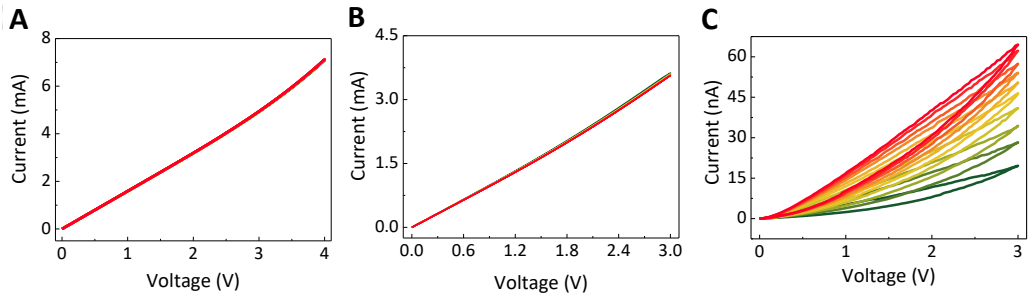

Fig. S4. Successive I-V curves in different 2D materials. I-V curves of (**A**) WTe_2, (**B**) 1T' $MoTe_2$, and (**C**) 2H-MoS_2 are shown. For WTe_2 and 1T' $MoTe_2$, there is no current/conductance variation induced by the sweeps.

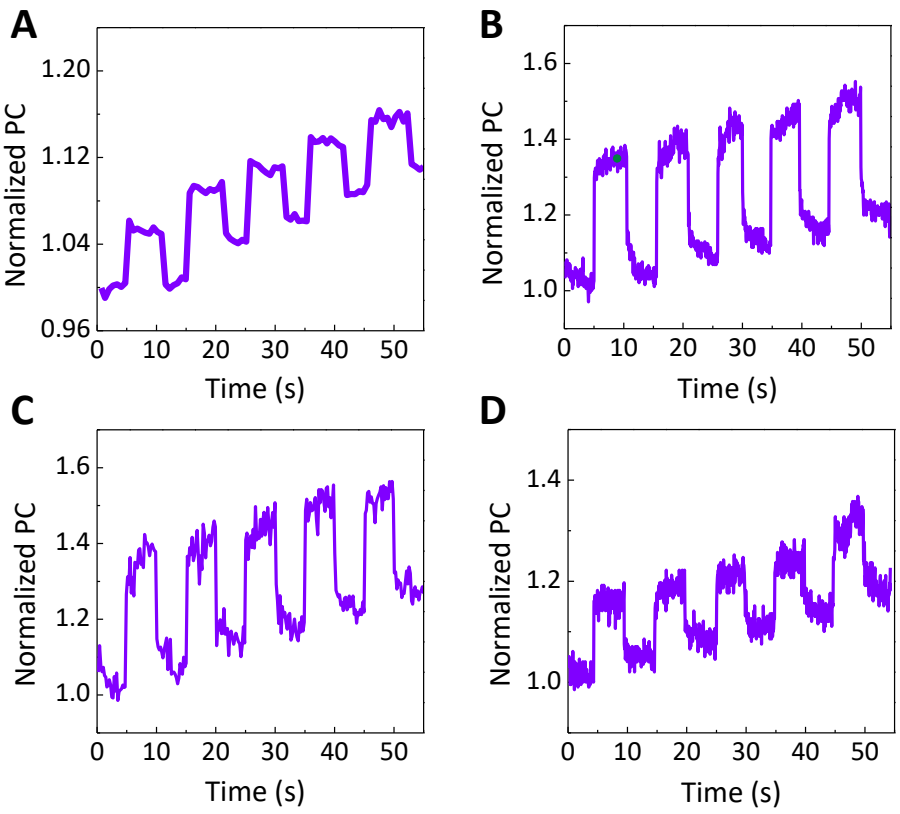

Fig. S5. Wavelength-dependent conductance variation under five successive optical pulse stimuli, at (**A**) 455nm, (**B**) 638nm, (**C**) 725nm, and (**D**) 811nm.

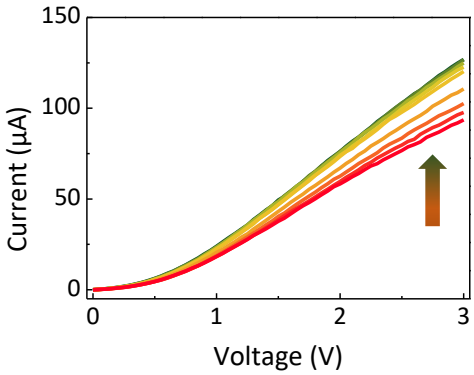

Fig. S6. Laser power-dependent photocurrents in SnS. The laser power values are increased from 83 μW to 43mW gradually.

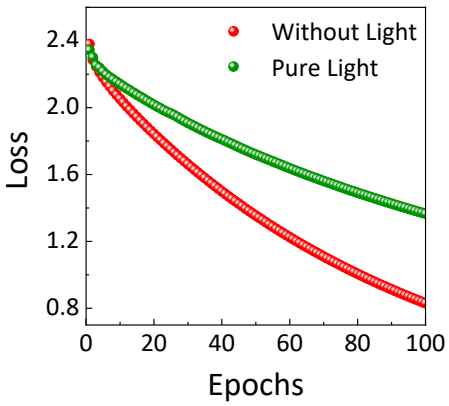

Fig. S7. Losses during the learning of the ten-class temporal inputs using the experimental reservoir states.

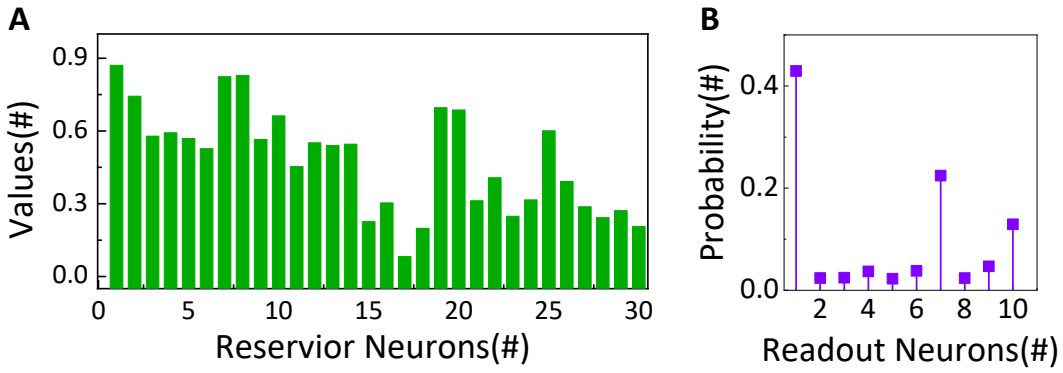

Fig. S8. Reservoir output and associated probability. An example of (A) the reservoir output and (B) the associated probability of readout neurons upon presenting the first type of letter as the input. The similarity between the first letter (“ㅏ”) and the seventh letter (“ㅁ”) can be recognized.

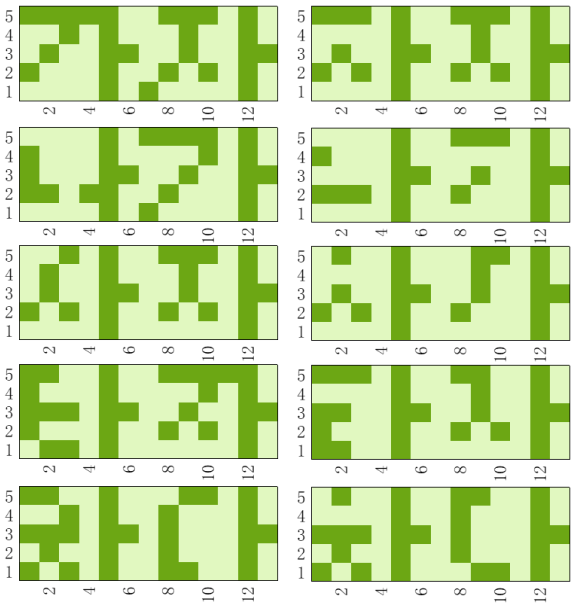

Fig. S9. Images for inference shown in Figure 4a with noise injected.

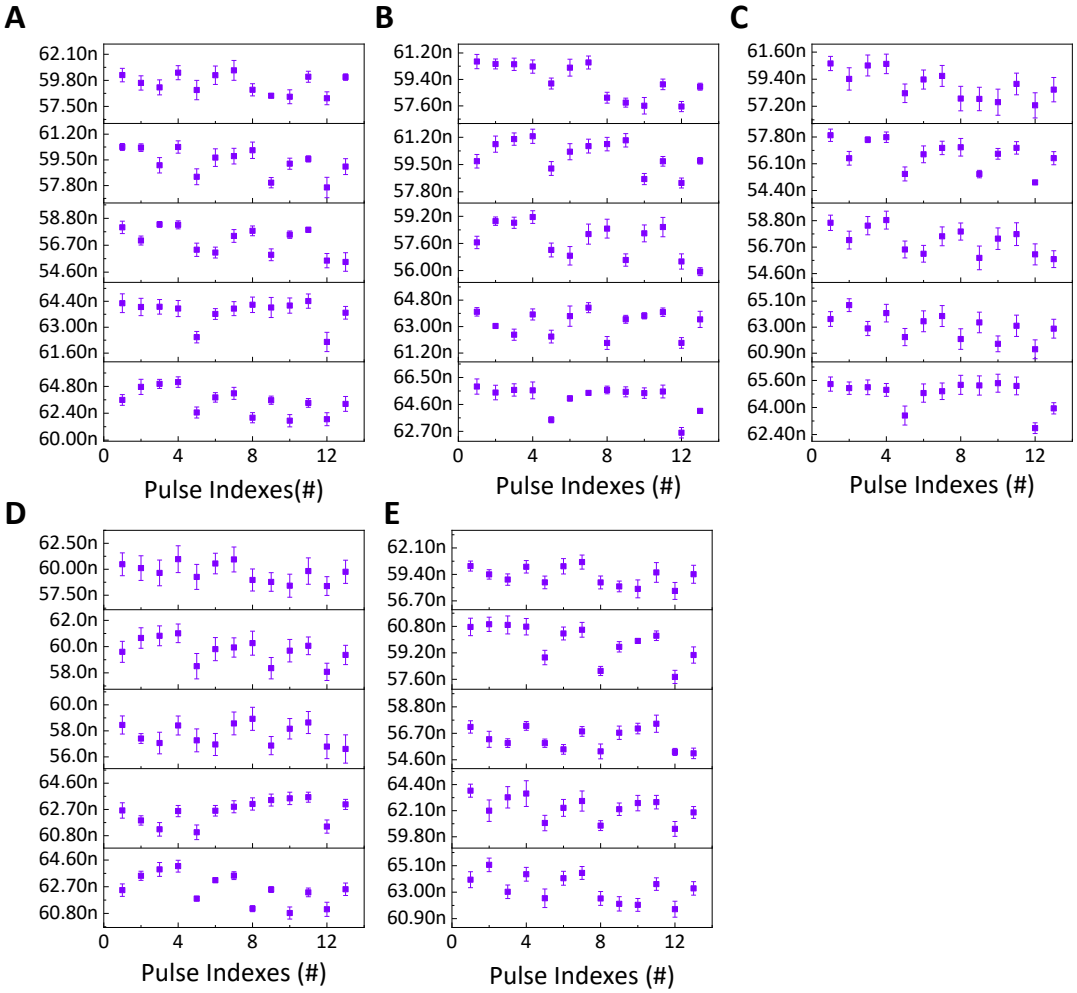

Fig. S10. The responses of memristors to the input signals after each stimulation. **(A)** 가자, **(B)** 나가, **(C)** 사자, **(D)** 타자, **(E)** 차다.

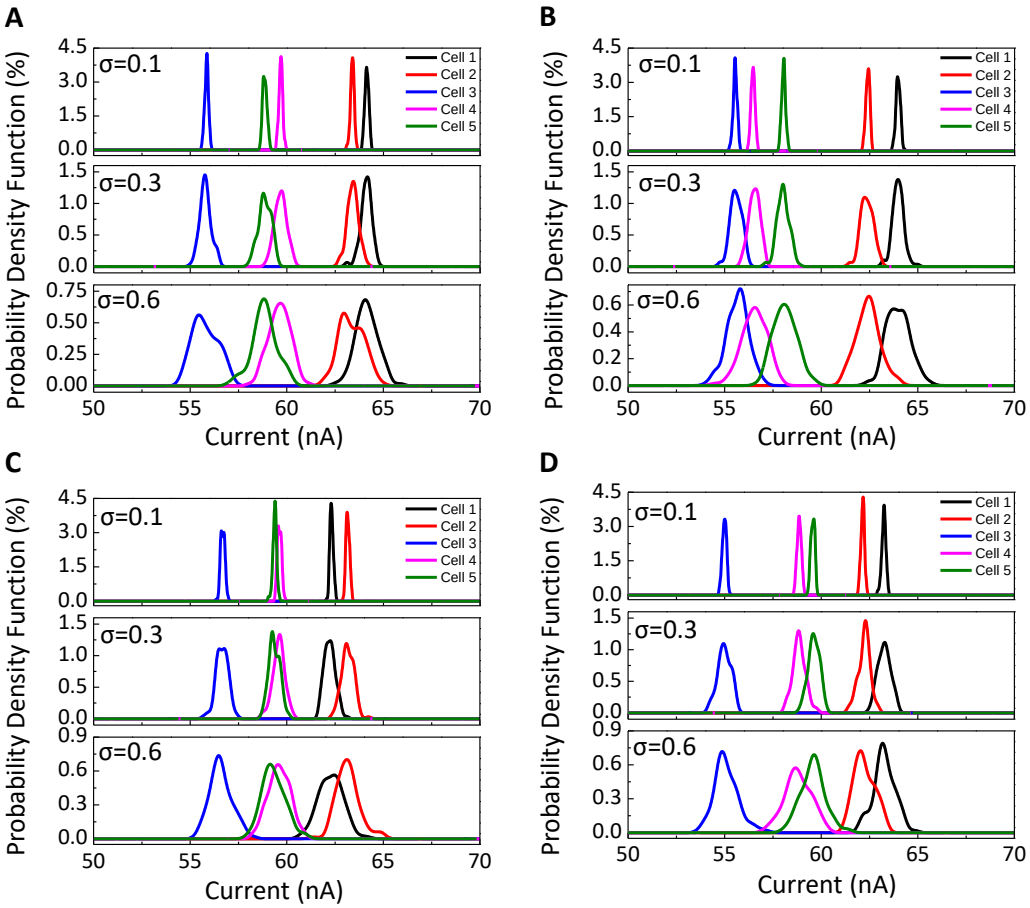

Fig. S11. Standard-deviation-dependent probability density function of the training data based on the experimental data sets. (A) 나가, (B) 사자, (C) 타자, and (D) 차다.

GIF Image 1. The evolution of the weights of readout layer within 100 epochs of electrical stimuli for Fig. 3.

GIF Image 2. The evolution of the weights of readout layer within 100 epochs of optical (b) stimuli for Fig. 3.

GIF Image 3. The evolution of the weights of readout layer within 100 epochs for Fig. 4.